Research Article | Vol. 25, No. 2 | 23 Jan 2017 | OPTICS EXPRESS 1360

Optics EXPRESS

All-order dispersion cancellation and energy-time entangled state

JINSOO RYU,[1,2] KIYOUNG CHO,[1] CHA-HWAN OH,[2] AND HOONSOO KANG[1,*]

[1]*Advanced Photonics Research Institute, Gwangju Institute of Science and Technology,123 cheomdangwagi-ro, Buk-gu, 500-712 Gwangju, South Korea*
[2]*Physics Department, Hanyang University, 222 Wangsimini-ro, Seongdong-gu, 04763 Seoul, South Korea*
[*]*hunskang@gist.ac.kr*

Abstract: Dispersion cancellation with an energy-time entangled photon pair in Hong-Ou-Mandel (HOM) interference is one phenomenon that reveals the nonclassical nature of the entangled photon pair. This phenomenon has been observed in materials with very weak dispersions. If the higher-order dispersion coefficient is non-negligible, then the experiment must be modified to realize dispersion cancellation. All-order dispersion cancellation using balanced dispersion was suggested by Steinberg. However, the same phenomenon is expected to occur even if a photon pair is not entangled. This behaviour can be explained by path indistinguishability with identical dispersion. To achieve an all-order dispersion experiment that cannot be explained classically, we modified the experiment and performed another all-order dispersion cancellation experiment that cannot be explained by identical dispersion. This is the first demonstration of nonclassical all-order dispersion cancellation.

OCIS codes: (270.0270) Quantum optics; (270.5530) Pulse propagation and temporal solitons.

References and links

1. A. Einstein, B. Podolsky, and N. Rosen, "B. Podolsky, and N. Rosen, "Can quantum-mechanical description of physical reality be considered complete?" Phys. Rev. **47**(10), 777–780 (1935).
2. J. C. Howell, R. S. Bennink, S. J. Bentley, and R. W. Boyd, "Realization of the Einstein-Podolsky-Rosen paradox using momentum- and position-entangled photons from spontaneous parametric down conversion," Phys. Rev. Lett. **92**(21), 210403 (2004).
3. T. B. Pittman, Y. H. Shih, D. V. Strekalov, and A. V. Sergienko, "Optical imaging by means of two-photon quantum entanglement," Phys. Rev. A **52**(5), R3429–R3432 (1995).
4. D. V. Strekalov, A. V. Sergienko, D. N. Klyshko, and Y. H. Shih, "Observation of two-photon "ghost" interference and diffraction," Phys. Rev. Lett. **74**(18), 3600–3603 (1995).
5. Y. Shih, "Entangled Photons," IEEE J. Sel. Top. Quantum Electron. **9**(6), 1455–1467 (2003).
6. Y. H. Shih, *An introduction to quantum optics*(CRC press,2011), Chap.12.
7. J. D. Franson, "Bell inequality for position and time," Phys. Rev. Lett. **62**(19), 2205–2208 (1989).
8. J. D. Franson, "Nonlocal cancellation of dispersion," Phys. Rev. A **45**(5), 3126–3132 (1992).
9. S. Y. Baek, Y. W. Cho, and Y. H. Kim, "Nonlocal dispersion cancellation using entangled photons," Opt. Express **17**(21), 19241–19252 (2009).
10. K. A. O'Donnell, "Observations of dispersion cancellation of entangled photon pairs," Phys. Rev. Lett. **106**(6), 063601 (2011).
11. T. Zhong and F. N. C. Wong, "Nonlocal cancellation of dispersion in Franson interferometry," Phys. Rev. A **88**(2), 020103 (2013).
12. C. K. Hong, Z. Y. Ou, and L. Mandel, "Measurement of subpicosecond time intervals between two photons by interference," Phys. Rev. Lett. **59**(18), 2044–2046 (1987).
13. A. M. Steinberg, P. G. Kwiat, and R. Y. Chiao, "Dispersion cancellation in a measurement of the single-photon propagation velocity in glass," Phys. Rev. Lett. **68**(16), 2421–2424 (1992).
14. M. C. Teich, B. E. Saleh, F. N. Wong, and J. H. Shapiro, "Variations on the theme of quantum optical coherence tomography: a review," Quantum Inform. Process. **11**(4), 903–923 (2012).
15. V. Giovannetti, S. Lloyd, L. Maccone, and F. N. C. Wong, "Clock synchronization with dispersion cancellation," Phys. Rev. Lett. **87**(11), 117902 (2001).
16. A. Valencia, G. Scarcelli, M. D'Angelo, and Y. Shih, "Two-photon imaging with thermal light," Phys. Rev. Lett. **94**(6), 063601 (2005).
17. R. S. Bennink, S. J. Bentley, R. W. Boyd, and J. C. Howell, "Quantum and classical coincidence imaging," Phys. Rev. Lett. **92**(3), 033601 (2004).

#280548 http://dx.doi.org/10.1364/OE.25.001360
Journal © 2017 Received 21 Nov 2016; accepted 30 Dec 2016; published 18 Jan 2017

Optics EXPRESS

18. G. Scarcelli, A. Valencia, and Y. Shih, "Two-photon interference with thermal light," Europhys. Lett. **68**(5), 618–624 (2004).
19. Y. S. Kim, O. Slattery, P. S. Kuo, and X. Tang, "Two-photon interference with continuous-wave multi-mode coherent light," Opt. Express **22**(3), 3611–3620 (2014).
20. J. Beugnon, M. P. Jones, J. Dingjan, B. Darquié, G. Messin, A. Browaeys, and P. Grangier, "Quantum interference between two single photons emitted by independently trapped atoms," Nature **440**(7085), 779–782 (2006).
21. R. Erdmann, D. Branning, W. Grice, and I. A. Walmsley, "Restoring dispersion cancellation for entangled photons produced by ultrashort pulses," Phys. Rev. A **62**(5), 053810 (2000).
22. R. K. Erdmann, Quantum interference engineered by dispersive parameter design," Ph.D Thesis, University of Rochester, 2004.
23. R. Okamoto, S. Takeuchi, and K. Sasaki, "Tailoring two-photon interference with phase dispersion," Phys. Rev. A **74**(1), 011801 (2006).
24. A. M. Steinberg, P. G. Kwiat, and R. Y. Chiao, "Dispersion cancellation and high-resolution time measurements in a fourth-order optical interferometer," Phys. Rev. A **45**(9), 6659–6665 (1992).
25. J. Garrison and R. Chiao, *Quantum Optics*(OUP, 2008), Chap. 10.
26. D. V. Strekalov, T. B. Pittman, and Y. H. Shih, "What we can learn about single photons in a two-photon interference experiment," Phys. Rev. A **57**(1), 567–570 (1998).
27. K. Cho and J. Noh, "Temporal ghost imaging of a time object, dispersion cancelation, and nonlocal time lens with bi-photon state," Opt. Commun. **285**(6), 1275–1282 (2012).
28. C. J. Broadbent, R. M. Camacho, R. Xin, and J. C. Howell, "Preservation of energy-time entanglement in a slow light medium," Phys. Rev. Lett. **100**(13), 133602 (2008).

1. Introduction

Since Einstein-Podolsky-Rosen [1] demonstrated that entanglement exists in quantum mechanics, the nonclassical nature of the entangled photon pair has been observed in various experiments. These experiments were realized with the position-momentum entangled photons [2–4] and also with the time-frequency entangled photon pair [5–15]. Whether these phenomena can be regarded as evidence that an entangled photon pair has properties that differ from those of classical light or a separable photon pair has been intensely debated [16–20].

To reveal the nonclassicality of the photon pair, an experiment should reflect a characteristic feature of the entangled system. The most characteristic feature of an energy-time entangled photon pair is that it has both strong temporal correlation and frequency anti-correlation

$$\Delta(t_s - t_i)\Delta(\omega_s + \omega_i - \omega_p) \le 1. \quad (1)$$

where t_s and t_i are the detection times of the signal and idler photons, respectively; and ω_s, ω_i ω_p are the angular frequencies of the signal, idler, and pump beam, respectively. This feature generates phenomena that are nonclassical and nonintuitive.

One phenomenon that reveals this nonclassical feature is dispersion cancellation. Two types of dispersion cancellation have been studied in quantum optics to date: the nonlocal dispersion cancellation of Franson, and the local dispersion cancellation of Steinberg [9–13]. Figure 1(a) and 1(b) demonstrate how the two dispersion cancellation types are nonintuitive. Figure 1(a) shows the nonlocal dispersion cancellation scheme of Franson. If two single-photon wave packets with strong temporal correlation pass through dispersive materials, their widths become broadened because of dispersion. In this case, the temporal correlation between the photons should be weakened. However, the temporal correlation is preserved in an experiment with an entangled photon pair. Figure 1(b) shows the local dispersion cancellation approach of Steinberg. A dispersive material is placed in one arm of the HOM interferometer. If two single-photon wave packets with strong temporal correlation pass through the interferometer, one wave packet becomes broadened. Thus, the two wave packets are no longer indistinguishable, and the visibility of the HOM interference will likely be reduced. However, the HOM interference pattern will not be changed, and only its position moves in an experiment with an energy-time entangled photon pair.

Optics EXPRESS

The frequency anti-correlation of the entangled pair cancels out the dispersion effect [8,13]. These dispersion cancellation phenomena can be realized only when the photon pair has both strong temporal correlation and strong frequency anti-correlation. Therefore, dispersion cancellation is one of the few phenomena that show the nonclassicality of the energy-time entangled photon pair. Without such a strong frequency anti-correlation, the HOM dip will be distorted [21].

However, Erdmann [22] also showed that the HOM dip can be restored in balanced dispersion without strong frequency anti-correlation. In such an experiment, photon pairs are generated via spontaneous parametric down-conversion (SPDC) using an ultrashort pump beam and balanced dispersion is realized with weak dispersion materials. For an ultrashort pump beam, the frequency anti-correlation between the signal and idler photons is very weak.

To realize both of the dispersion cancellation schemes of Steinberg and Franson, the dispersion of the medium should be so weak that the dispersion relation can be approximated to the second-order coefficient. If higher-order coefficients are non-negligible, those dispersion cancellation schemes are no longer valid. For example, Okamoto et al. [23] showed that the HOM dip is clearly distorted when the dispersion cancellation method of Steinberg is attempted with a strongly dispersive medium.

Steinberg suggested that all-order dispersion cancellation [24], i.e., the compensation of both the even-order dispersion and odd-order dispersion of higher-order coefficients, might be realized by balanced dispersion. If an identical medium is placed in both arms of the HOM interferometer, odd-order dispersion is cancelled by the frequency anti-correlation of the entangled photon pair. In contrast, even-order dispersion is cancelled because of the original nature of the HOM interference [13,25]. Similar to the experiment of Erdmann [22], this all-order dispersion cancellation is expected to occur even without strong frequency correlation. As an extreme case, according to our theoretical considerations, the original HOM dip can be restored in balanced dispersion with an independent and separable photon pair with strong temporal correlation (see Appendix B).

In this case, the two photons are not entangled, and there is no frequency anti-correlation.

It is the indistinguishability of the wave packet after identical dispersion that restores the original HOM dip. In other words, all-order dispersion cancellation in HOM interference can be realized both with and without frequency anti-correlation. This is the reason that the nonclassicality of an entangled photon pair cannot be observed in this type of all-order dispersion cancellation.

Therefore, we considered an all-order dispersion cancellation experiment that can be realized only with an energy-time entangled photon pair (Fig. 1(d)). If a Mach-Zender interferometer is added to the HOM interferometer, then single-photon wave packets with classical temporal correlation cannot explain the interference pattern [26]. If balanced dispersion materials are placed in this interferometer, the restoration of the HOM interference pattern in this system cannot be explained by identical dispersion. Indeed, only two-photon temporal coherence and frequency anti-correlation can explain this effect. We will show that all-order dispersion cancellation in a modified HOM interferometer is one of few phenomena that demonstrate the nonclassicality of the energy-time entangled state.

In the next section, we will explain in detail the principle of all-order dispersion cancellation in a HOM interferometer with an energy-time entangled photon pair. We will also explain why all-order dispersion cancellation in a modified HOM interferometer requires energy-time entanglement but cannot be realized with a separable photon pair with strong temporal correlation.

In the **Experiment** section, we will present how all-order dispersion cancellation can be realized experimentally. We will also show the distortion and restoration of the HOM interference pattern in terms of the change of the dispersion balance of the signal and idler photons.

Optics EXPRESS

2. Balanced dispersion and all-order dispersion cancellation

If a pump beam with angular frequency ω_p generates a photon pair via SPDC and if the angular frequency of the signal photon is ω_s and the angular frequency of idler photon is ω_i, the quantum state of the photon pair can be written as [5,6,27]

$$\begin{aligned}|\Psi\rangle &= \iint d\omega_s d\omega_i f(\omega_s,\omega_i)\delta(\omega_p-\omega_s+\omega_i)\hat{a}_s^\dagger(\omega_s)\hat{a}_i^\dagger(\omega_i)|0\rangle \\ &= \iint d\mu_s d\mu_i f'(\mu_s,\mu_i)\delta(\mu_s+\mu_i)\hat{a}_s^\dagger(\omega_s^0+\mu_s)\hat{a}_i^\dagger(\omega_i^0+\mu_i)|0\rangle. \\ &= \int d\mu_s F(\mu_s)\hat{a}_s^\dagger(\omega_s^0+\mu_s)\hat{a}_i^\dagger(\omega_i^0-\mu_s)|0\rangle\end{aligned} \quad (2)$$

with $\mu_s=\omega_s-\omega_s^0, \mu_i=\omega_i-\omega_i^0, \omega_s^0=\omega_i^0=\omega_p/2$ and $f'(\mu_s,\mu_i)=f(\omega_s^0+\mu_s,\omega_i^0+\mu_i)$, $F(\mu_s)=f'(\mu_s,-\mu_s)$.

This photon pair passes through a dispersive medium with a dispersion relation of the following form:

$$\begin{aligned}k(\omega) &= k(\omega_0)+\left.\frac{d\omega}{dk}\right|_{\omega_0}(\omega-\omega_0)+\frac{1}{2}\left.\frac{d^2\omega}{dk^2}\right|_{\omega_0}(\omega-\omega_0)^2+\ldots \\ &= k(\omega_0)+\alpha(\omega-\omega_0)+\beta(\omega-\omega_0)^2\ldots\end{aligned} \quad (3)$$

where $\alpha=\left.\frac{d\omega}{dk}\right|_{\omega_0}, \beta=\frac{1}{2}\left.\frac{d^2\omega}{dk^2}\right|_{\omega_0}$. α is the reciprocal of the group velocity, and β is related to the dispersion of the group velocity.

Steinberg's dispersion cancellation experiment showed that if a weakly dispersive medium is

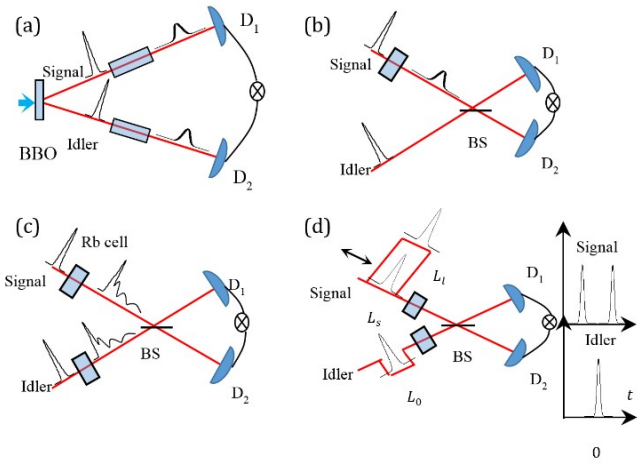

Fig. 1. Nonclassicality of dispersion cancellation.(a) Nonlocal dispersion cancellation of Franson. Signal and idler photons pass through dispersive materials with opposite dispersion coefficients. The temporal correlation between the signal and idler photons is preserved. (b) Local dispersion cancellation of Steinberg. A dispersive material is placed in the path of a signal photon. The shape of the HOM dip is preserved, and only the position of the dip is shifted. (c) All-order dispersion cancellation with balanced dispersion. Identical dispersive materials are placed in the paths of the signal photon and the idler photon. Even if the material has an arbitrary dispersion property, the HOM dip will be preserved. (d) Balanced dispersion with a modified HOM interferometer. The Mach-Zender interferometer is placed in one path of the interferometer in (c).

Optics EXPRESS

placed in the path of the signal photon, then the HOM dip is not distorted, and only its position is shifted. The term "Weakly dispersive" describes the case in which the dispersion relation can be approximated to the second-order coefficient β. The HOM interference dip without a dispersive medium is given by

$$P_{12} = \frac{1}{2}\int_{-\infty}^{\infty} d\mu \left|F(\mu)\right|^2 \left(1-\cos\left(2\mu\frac{\Delta L}{c}\right)\right) = \frac{1}{2}\left(1-\int_{-\infty}^{\infty} d\mu \left|F(\mu)\right|^2 \cos\left(2\mu\frac{\Delta L}{c}\right)\right). \tag{4}$$

when we rewrite all the detuning as μ. ΔL is the path length difference between signal path and idler path. The HOM dip with a dispersive medium in Steinberg's dispersion cancellation is modified to

$$P_{12} = \frac{1}{2}\int_{-\infty}^{\infty} d\mu \left|F(\mu)\right|^2 \left(1-\cos\left(2\mu\left(\frac{\Delta L - L}{c}+\alpha L\right)\right)\right) = \frac{1}{2}\left(1-\int_{-\infty}^{\infty} d\mu \left|F(\mu)\right|^2 \cos\left(2\mu\left(\frac{\Delta L - L}{c}+\alpha L\right)\right)\right). \tag{5}$$

where L is the length of the dispersive medium (see Appendix A). The shape of the dip is not changed, and only the position of the dip is shifted [13,26]. However, this process is only valid when the dispersion relation can be approximated to the second-order coefficient. If higher-order terms are non-negligible, the dispersion cancellation effect mentioned above is not valid.

For example, if we consider the dispersion relation up to the third-order term, we have

$$k_s(\mu) = k_0 + \alpha_s\mu + \beta_s\mu^2 + \gamma_s\mu^3 + \ldots \qquad k_s(-\mu) = k_0 - \alpha_s\mu + \beta_s\mu^2 - \gamma_s\mu^3 + \ldots \tag{6}$$

and the HOM dip is modified to

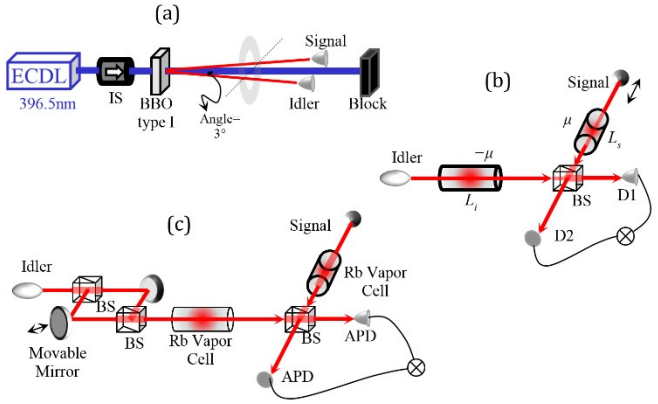

Fig. 2. Experimental setups. (a) Signal and idler photons are generated via SPDC. The two photons are energy-time entangled. (b) HOM interference with balanced dispersion. Both signal and idler photons pass through respective Rb vapour cells and are then detected by a Single-photon Avalanche Detector (SPAD, Perkin Elmer SPCM-AQRH-1X). At the same temperature, the dispersion properties of the two cells are identical. (c) Balanced dispersion in a modified HOM interferometer. Mach-Zender interferometer is placed in one arm of the interferometer.

Optics EXPRESS

$$P_{12} = \frac{1}{2}\int_{-\infty}^{\infty} d\mu |F(\mu)|^2 \left(1-\cos\left(2\mu\left(\frac{\Delta L - L}{c} + (\alpha + \gamma\mu^2)L\right)\right)\right)$$
$$= \frac{1}{2}\left(1-\int_{-\infty}^{\infty} d\mu |F(\mu)|^2 \cos\left(2\mu\left(\frac{\Delta L - L}{c} + (\alpha + \gamma\mu^2)L\right)\right)\right). \quad (7)$$

The phase differences from odd-order terms are not cancelled out, and the path difference for complete destructive interference depends on the frequency of the signal photon. As a result, the HOM dip is distorted. The experiment of Okamoto et.al [23] shows this phenomenon very well. A solution for this problem was previously suggested by Steinberg [24].

Suppose that the signal and idler photons with detuning $\mu, -\mu$ each pass through a dispersive medium, as shown in Fig. 2(b). If we express the dispersion relation to the third-order dispersion coefficient, we have

$$k_s(\mu) = k_0 + \alpha_s\mu + \beta_s\mu^2 + \gamma_s\mu^3 + \ldots$$
$$k_i(-\mu) = k_0 - \alpha_i\mu + \beta_i\mu^2 - \gamma_i\mu^3 + \ldots \quad . \quad (8)$$

The phase change of the whole quantum state is the sum of the phase changes for the signal and idler photons. If the signal and idler photons travel the same distance in a dispersive medium, the phase changes are proportional to $k_s(\mu) + k_i(-\mu)$ and are expanded as follows:

$$k_s(\mu) + k_i(-\mu) = 2k_0 + (\alpha_s - \alpha_i)\mu + (\beta_s + \beta_i)\mu^2 + (\gamma_s - \gamma_i)\mu^3 + \ldots \quad . \quad (9)$$

If two dispersive media have the same dispersion coefficients, then all the odd-order terms are cancelled out:

$$k_s(\mu) + k_i(-\mu) = 2k_0 + 2\beta_s\mu^2 + \ldots \quad . \quad (10)$$

Therefore, the quantum state for the frequency pair becomes

$$|\psi\rangle_{\mu,-\mu} = |\mu\rangle_s |-\mu\rangle_i$$
$$|\psi'\rangle_{\mu,-\mu} = \exp[i(k_s(\mu) + k_i(-\mu)L)]|\mu\rangle_s |-\mu\rangle_i$$
$$= \exp 2i[k_0 + 2\beta_s\mu^2]|\mu\rangle_s |-\mu\rangle_i$$
$$|\psi'\rangle_{-\mu,\mu} = \exp 2i[k_0 + 2\beta_s\mu^2]|-\mu\rangle_s |\mu\rangle_i \quad . \quad (11)$$

,if we approximate even order terms to the second order coefficient. If the photons of the photon pair in this quantum state meet at the beam splitter, HOM interference occurs, and even-order dispersion cancellation is achieved. The same principle is applied to the higher-order terms. Based on these processes, all-order dispersion cancellation, in which both the odd-order dispersion effect and the even-order dispersion effect are cancelled, is realized.

However, the recovery of the HOM interference pattern can also be achieved with a photon pair without energy-time entanglement. As explained in the Appendix B, the same phenomenon is expected to occur when the entangled pair is replaced with separable single photons exhibiting strong temporal correlation. If the two wave packets pass through a balanced dispersion HOM interferometer, then the original interference pattern can be restored. Thus, all-order dispersion cancellation in a HOM interferometer can be realized with or without energy-time entanglement.

To reveal the nonintuitive or nonclassical nature of an entangled photon pair with all-order dispersion cancellation, we devised another experiment. This type of phenomenon can be realized by using HOM interference that cannot be explained with two separable single-

Optics EXPRESS

photon wave packets. This nonclassical behaviour can be achieved using a balanced dispersion HOM interferometer with a Mach-Zender interferometer in the path of the idler photon, as shown in Fig. 3. In [26], HOM interference that can be explained only by biphoton interference was observed. A Mach-Zender interferometer was inserted in one arm of the HOM interferometer in the experiment of [26]. Using this approach, an explanation of the interference pattern based on the indistinguishability of two identical single photon wave packet was excluded. If an identical dispersive medium (atomic cell) is placed in each arm of the interferometer, then the experimental setup becomes the same as that of the experiment presented in Fig. 3(a).

In the setup of Fig. 3(a), the signal photon can pass through both the long path and the short path. When $L_o = (L_{Long} + L_{Short})/2$, if the idler photon travels along the long path, it travels a longer distance than the signal photon. The interference of a dispersed biphoton wave packet can be analysed using a method similar to that described in [26].;Suppose that a photon is detected at D_1 at time t_1 and that another photon is detected at D_2 at time t_2. We investigate the interference that determines the probability of this event. Following Strekalov et al., we introduce the concept of an "effective photon wave function", which is defined as

$$\psi(t_1,t_2) = \langle 0 | \hat{E}_1^{(+)}(t_1)\hat{E}_2^{(+)}(t_2) | \Psi \rangle, \tag{12}$$

where $|\Psi\rangle$ is the quantum state of the entangled photon pair [6,24]. If we define the

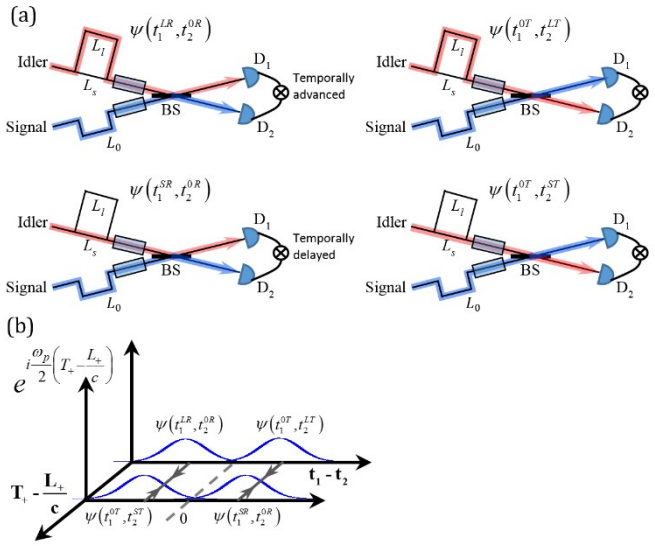

Fig. 3. Two-photon interference in a modified HOM interferometer with balanced dispersion. When photons are detected at D_1 and D_2, the two photons could have originated from four indistinguishable paths. The temporally advanced two-photon detection amplitude can be transmitted or reflected at the beam splitter. The temporally delayed amplitude also can be transmitted or reflected at the beam splitter. . Since the signal photon path length for the amplitude generated earlier is relatively long, the amplitudes can interfere at the detectors. The coincidence count when $L_o = (L_{Long} + L_{Short})/2$ is determined by this interference. The effective photon wave function corresponding to each path is marked. (b) Biphoton wave packet after balanced dispersion. Only the width of the wave packet is increased via even-order dispersion. The effective two-photon wave functions corresponding to the paths in (a) are drawn in the temporal domain. Wave packets connected by the arrows are pairs that interfere when $L_o = (L_{Long} + L_{Short})/2$. If the phase difference between them is π, they interfere destructively, resulting in a dip. If the phase difference is 0, they interfere constructively, generating a peak. $T_+ = t_1 + t_2$ and L_+ denotes sum of signal path length and idler path length. $L_+ = L_s + L_i$.

Optics EXPRESS

effective wave function to detect photons as $\psi_{12}(t_1,t_2)$, we can obtain the following:

$$\psi_{12}(t_1,t_2)=\psi(t_1^{0T},t_2^{LT})+\psi(t_1^{LR},t_2^{0R})+\psi(t_1^{0T},t_2^{ST})+\psi(t_1^{SR},t_2^{0R}). \quad (13)$$

LT indicates that the idler photon passes through the long arm of the MZ interferometer and is transmitted at the beam splitter. 0T indicates that the signal photon passes through the L_0 path and is transmitted at the beam splitter. 0R indicates that the signal photon passes the L_0 path and is reflected at the beam splitter. SR indicates that the idler photon passes through the short arm of the MZ interferometer and is reflected at the beam splitter [6,26].

Interference between those four effective photon wave functions generates a dip or peak at the central position. Figure 3(b) shows this interference between effective two-photon wave functions in the temporal domain. If the signal photon follows the short path, it travels a distance shorter than that travelled by the idler. Both the signal and idler photons pass through their respective atomic cells; thus, odd-order dispersion is cancelled, and only even-order dispersion remains. The distribution of the biphoton wave packet is shown in Fig. 3(c). The two dispersed wave packets corresponding to the short and long signal paths are overlapped. If $L_o = (L_{Long} + L_{Short})/2$, the dispersed wave packet of $\psi(t_1^{LT},t_2^{0T})$ and the wave packet of the $\psi(t_1^{0R},t_2^{SR})$ path can be overlapped and interfere (T denotes transmission, and R indicates reflection). Because the two wave packets are generated at different times in the SPDC crystal, they have different overall phases. This phase difference resulting from the generation time difference is determined by the MZ interferometer. The interference terms also depend on this phase difference.

The signal and idler each pass through an identical Rb cell. When the temperatures of both cells are the same, then the odd-order dispersion is cancelled out by frequency anti-correlation. Similar to the case of an unmodified HOM interferometer, even-order dispersion does not change the HOM interference pattern. Therefore, the original interference pattern without a dispersive medium is restored, and all-order dispersion cancellation is realized.

This phenomenon cannot be explained as interference between two identical single-photon wave packets. If two separable wave packets pass through this modified HOM interferometer, as shown in Fig. 1(d), then the wave packet of the signal photon is modified. After passing through a dispersive medium, the wave packets of both the signal and idler photons are dispersed and spread out. These two wave packets cannot be overlapped at the beam splitter (BS). In other words, the restoration of the central dip or peak in the modified HOM interferometer with balanced dispersion can be achieved only with an entangled photon pair. The formation of the central dip or peak is possible because of two-photon temporal coherence. The temporal coherence originates from frequency anti-correlation. Additionally, odd-order dispersion is cancelled nonlocally because of frequency anti-correlation. All-order dispersion cancellation in the modified HOM interferometer requires both strong temporal correlation and strong frequency anti-correlation. The nonclassical nature of the entangled photon pair is revealed by this process.

3. Experiment

The goals of the experiments are to realize all-order dispersion cancellation and reveal its nonclassical nature. As a preliminary experiment, we achieved all-order dispersion cancellation using two identical dispersive media—one in the signal path and the other in the idler path of the HOM interferometer—as suggested by Steinberg [24]. This experiment shows that the HOM dip is distorted when the dispersion is unbalanced and that, for balanced dispersion, the original dip is restored.

In this experiment, the pulse broadening of a Gaussian wave packet in a dispersive medium can be calculated as

Optics EXPRESS

$$\int_{-\infty}^{\infty} d\omega \frac{1}{\Delta\omega\sqrt{2\pi}} e^{-\frac{(\omega-\omega_0)^2}{2(\Delta\omega)^2}} e^{i\frac{\omega}{c}(n(\omega)-1)L_{cell}} e^{-i\omega t}. \quad (14)$$

Figure 4 shows how the calculated envelope of a Gaussian pulse (full width at half maximum [FWHM] = 3 nm) is distorted in the Rb vapour cells with temperatures of 60°C and 140°C. As Shown by the large asymmetry of wave packet in Fig. 4, the distortion caused by the odd-order dispersion coefficient is very high in the Rb vapour cell at 140°C. Therefore, unlike Steinberg's experiment [13], dispersion cancellation cannot be realized in experiment 1 if the dispersive medium is placed in only one arm of the interferometer. Identical dispersive media (Rb cells at the same temperature), one placed in each arm of the interferometer, were used to achieve all-order dispersion cancellation.

Figure 5(a) shows the experimental result. The temperature of the Rb cell in the signal-photon path is fixed at 140°C. The temperature of the Rb cell in the idler path is varied (142, 144, 146, 148, and 150°C). The HOM dip for each case is shown in the figure. At 142 and 144°C, the side peak (dip) resides to the left of the main dip. At 148 and 150°C, a waving pattern can be observed to the right of the main dip. At 146°C, the waving pattern disappears from both sides and the HOM dip without dispersion is restored

This result confirmed that dispersion cancellation cannot be realized by placing a Rb hot vapour cell in only one arm, as in Steinberg's dispersion cancellation approach. We also verified that all-order dispersion cancellation is achieved when a balanced dispersion material is placed in the idler path. The temperatures of two cells are not exactly the same when the HOM dip is restored because a constant difference exists between the nominal temperatures of the temperature sensor and the actual temperature of the Rb cell. As shown in Fig. 5(b), if we increase the temperature of the Rb cell in the idler path, the visibility of the HOM dip gradually increases and is almost completely restored at exactly 146°C. If the temperature is further increased, however, the visibility decreases again.

Although this experiment shows that the HOM dip is restored, the nonclassicality of the energy-time entangled photon pair is not revealed in the experiment because it can also be realized with an identical dispersion of separable pulses (see Appendix B). Thus, another experiment must be devised to reveal the nonclassical nature of the entangled photon in all-order dispersion cancellation. Thus, we realized all-order dispersion cancellation with a modified HOM interferometer. As in the experiment by Strekalov et al. [26], a Mach-Zender interferometer is placed in the idler path of the HOM interferometer. The Mach-Zender interferometer is unbalanced, and the path length difference is 600μm. Identical dispersion media are used: one placed in the signal arm and the other in the idler arm. The bandwidth of

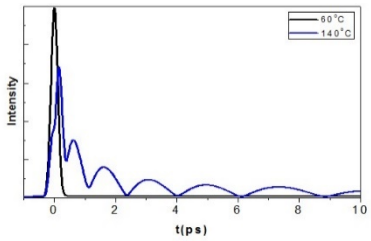

Fig. 4. Distortion of a wave packet by dispersion. If a Gaussian pulse passes through a Rb cell, its shape becomes distorted because of dispersion. At 60°C, the effect of dispersion is negligible, whereas at 140°C, the Gaussian wave packet is clearly distorted. After dispersion, the wave packet is highly asymmetric, and the width of the wave packet is increased by more than 10 times.

Optics EXPRESS

the idler photon is 3nm by post selection, and the corresponding coherence length is ~140μm. The path length difference is several times longer than the coherence length. Thus, single-photon interference is avoided.

In the absence of the dispersion effect, the interference pattern is similar to that shown in Fig. 5(c). The HOM dips of the short and long paths reside in the left and right sides of the pattern, respectively. In the centre of the pattern, a dip (or peak) generated from the phase difference between the short and long paths of the MZ interferometer is observed.

As explained previously, the peak or dip in the centre cannot be explained by the overlap of the wave packets of the signal and idler photons, i.e., if this peak or dip is restored, we can explain this phenomenon only by the frequency anti-correlation of an entangled photon pair. The original interference pattern (black line) is observed when the temperatures of both cells are 20°C. The dispersion effect is negligible at this temperature, as shown in Fig. 4. When one of the cells is heated to 140°C, dispersion occurs only in the cell. In this case, the dispersion is not balanced, and the interference pattern is distorted (red line) from the original interference pattern (black line). When the temperature of another cell is also increased to 140°C, balanced dispersion is achieved. In this case, the original interference pattern is clearly restored (blue line). This phenomenon can be treated more quantitatively. The distortion of the two-photon interference pattern reflects the odd-order dispersion of a biphoton wave packet. We can determine the degree of odd-order dispersion based on the visibility of the interference dip or peak. As shown in Fig. 4, asymmetric distortion occurs via odd-order dispersion. Thus, the degree of asymmetry reflects how much odd-order dispersion occurred. To measure the degree of asymmetry, we can decompose a biphoton wave packet to a symmetric function and an anti-symmetric function. If the probability for the symmetric function is P_S and the probability for the anti-symmetric function is P_A, the quantity, $D.A. = 1 - |P_S - P_A|$, reflects the degree of asymmetry. For asymmetric wave functions, $D.A. > 0$. More asymmetric functions are correlated with higher $D.A.$ values. The visibility cannot be $V = 1$ if the wave function is asymmetric. For a more asymmetric wave function, the visibility has a smaller value. $D.A.$ can be calculated as $D.A. = 1 - V$ (see Appendix C).

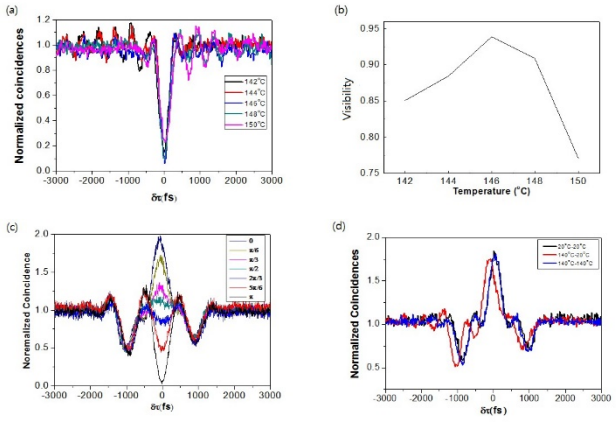

Fig. 5. Distortion and restoration of HOM interference pattern. (a) HOM interference patterns for different RB cell temperatur-es. The temperature of the Rb cell in the idler path is varied (142-150°C), whereas the temperature of the Rb cell in the signal-photon path is fixed at 140°C. (b) Visibility of the HOM dip. The visibility depends on the temperature of the Rb cell in the idler path. (c) Two-photon interference pattern in the modified HOM interferometer. As the phase difference changes in the Mach-Zender interferometer, the interference pattern near position 0 changes from a dip to a peak. (d) Restoration of the two-photon interference pattern in the modified HOM interferometer with balanced dispersion. The phase difference between the short and long paths in MZI is 0, and a peak is generated by interference.

Optics EXPRESS

Figure 5(b) shows the change in the visibility at different Rb cell temperatures. At 142°C, the visibility is 0.85, and the *D.A.* is 0.15. At 146°C, the visibility increases to 0.94, and the *D.A.* decreases to 0.06. At 150°C, the visibility decreases further to 0.77, and the *D.A.* increases to 0.23. These trends reveal the change in the wave function asymmetry caused by changing the temperature.

The modified HOM interference can be analysed similarly (see Appendix D). For the curve of Fig. 5(d), $V = 0.8150$ at low temperature (60°C). The maximum visibility without dispersion in Fig. 5. (d) is less than that of the interference pattern without the Rb cell in Fig. 5(c) because mode matching is imperfect in the experiment shown in Fig. 2(c). The Rb cell geometry is not ideal for beam alignment. The two signal beams in the MZ interferometer also travel different distances. When these effects are combined, it is difficult to realize perfect mode matching. Therefore, $V = 0.8150$, even when the biphoton wave packet should have perfect symmetry. Furthermore, $D.A. = 0.1850$ if we apply the formula $D.A. = 1 - V$. When the idler cell temperature is increased to 140°C, the visibility decreases to $V = 0.7150$, and the *D.A.* increases to $D.A. = 0.2850$. When the signal cell temperature is also increased to 140°C, the visibility increases further to $V = 0.8409$, and the *D.A.* decreases to 0.1591.

4. Methods

The entangled photon source was prepared by injecting a 396.5-nm pump beam into a type I beta barium borate (BBO) crystal. The centre frequencies of the signal and idler photons are both 793 nm, and the line width is 3 nm. Each photon passes through a Rb vapour cell with strong dispersion (i.e., high-order dispersion coefficients cannot be neglected). The Rb atom has a D1 transition line near 795 nm, and the refractive index is given as

$$n(\omega) = \int_{-\infty}^{\infty} d\omega G(\omega) \left[1 - \sum_{j=1}^{2} \frac{N|\mu_j|^2}{2\varepsilon h} \sum_{k=1}^{4} \frac{g_{jk}}{\omega - \omega_{jk} + i(\gamma_j + \gamma_c)} \right]. \quad (15)$$

where $j = \{1,2\} \rightarrow \{Rb_{85}, Rb_{87}\}$, $k = \{1,2,3,4\} \rightarrow \{$if $j = 1$ $F = 2 \rightarrow F' = 2$, $F = 2 \rightarrow F' = 3$, $F = 3 \rightarrow F' = 2$, $F = 3 \rightarrow F' = 3\}$, $\{j = 2$ $F = 1 \rightarrow F' = 1$, $F = 1 \rightarrow F' = 2$, $F = 2 \rightarrow F' = 1$, $F = 2 \rightarrow F' = 2\}$, and $G(\omega_i)$ is the Doppler convolution function. μ_j is the dipole moment, g_{jk} is the relative peak strength, and N is the atomic number density [28].

Because the path length difference changes slightly because of mechanical vibration, the phase also changes continuously in the modified HOM interferometer. To fix the phase, Piezo-electric Transducer (PZT) is attached to the mirror in the long path of the Mach-Zender interferometer. The Mach-Zender interference signal of a reference laser (a He-Ne laser) was used to detect the error signal. Low-frequency noise is eliminated (≤ 300 Hz) by adding a voltage from the He-Ne laser error signal-detection system to the PZT. The PZT is proportional-integral (PI) controlled.

5. Conclusion

The nonlocal dispersion cancellation method of Franson and the local dispersion cancellation method of Steinberg reveal the nonclassical nature of an energy-time entangled state. Those nonclassical phenomena can be realized only when a photon pair has both strong temporal correlation and strong frequency anti-correlation. Both dispersion cancellation schemes can be achieved only when the dispersion coefficients can be approximated to the second order. Different methods are required to obtain all-order dispersion cancellation. Therefore, we achieved all-order dispersion cancellation using balanced dispersion with HOM. This phenomenon, however, is possible even without energy-time entanglement. Thus, the HOM dip can be restored without dispersion, even if two photons are independent and separable. The indistinguishability from identical dispersion restores the original HOM dip.

Optics EXPRESS

Thus, we restored the HOM interference pattern using a modified HOM interferometer with a Mach-Zender interferometer. This finding can be explained only by considering both temporal correlation and frequency anti-correlation. Therefore, the nonclassical nature of an energy-time entangled system can be revealed, even if the dispersive material has an arbitrary dispersion property.

Appendix A: Hong-Ou-Mandel (HOM) interference and second order dispersion cancellation with an energy-time entangled photon pair

Dispersion cancellation of Steinberg [13] is schematically shown in Fig. 6(a). The dispersion relation can be approximated to the second-order dispersion coefficient for a glass sample. If this glass is placed in the idler path of the HOM interferometer, the HOM dip is not distorted, and only its position is shifted. If a pump beam with angular frequency ω_p generates a photon pair via spontaneous parametric down conversion(SPDC) and if the angular frequency of the signal photon is ω_s and the angular frequency of the idler photon ω_i, the quantum state of the photon pair can be written as [5,6,27]

$$\begin{aligned}|\Psi\rangle &= \iint d\omega_s d\omega_i f(\omega_s,\omega_i)\delta(\omega_p-\omega_s+\omega_i)\hat{a}_s^\dagger(\omega_s)\hat{a}_i^\dagger(\omega_i)|0\rangle \\ &= \iint d\mu_s d\mu_i f'(\mu_s,\mu_i)\delta(\mu_s+\mu_i)\hat{a}_s^\dagger(\omega_s^0+\mu_s)\hat{a}_i^\dagger(\omega_i^0+\mu_i)|0\rangle. \\ &= \int d\mu_s F(\mu_s)\hat{a}_s^\dagger(\omega_s^0+\mu_s)\hat{a}_i^\dagger(\omega_i^0-\mu_s)|0\rangle\end{aligned} \tag{16}$$

with $\mu_s=\omega_s-\omega_s^0, \mu_i=\omega_i-\omega_i^0, \omega_s^0=\omega_i^0=\omega_p/2$

and $f'(\mu_s,\mu_i)=f(\omega_s^0+\mu_s,\omega_i^0+\mu_i)$, $F(\mu_s)=f'(\mu_s,-\mu_s)$

This photon pair passes through a dispersive medium with a dispersion relation of the following form:

$$\begin{aligned}k(\omega) &= k(\omega_0)+\left.\frac{d\omega}{dk}\right|_{\omega_0}(\omega-\omega_0)+\frac{1}{2}\left.\frac{d^2\omega}{dk^2}\right|_{\omega_0}(\omega-\omega_0)^2+\ldots \\ &= k(\omega_0)+\alpha\mu+\beta\mu^2+\ldots\end{aligned} \tag{17}$$

$\mu = \omega-\omega_0$ and $\alpha=\left.\frac{d\omega}{dk}\right|_{\omega_0}, \beta=\frac{1}{2}\left.\frac{d^2\omega}{dk^2}\right|_{\omega_0}$ where α is the reciprocal of the group velocity, and β is related to the dispersion of the group velocity. If this dispersive medium is placed in the path of the signal photon, the magnitudes of wave vector of the signal photon with detuning μ and detuning $-\mu$ become

$$\begin{aligned}k_0 &= \omega_s^0/c \\ k_s(\mu) &= k_0+\alpha\mu+\beta\mu^2+\ldots \\ k_s(-\mu) &= k_0-\alpha\mu+\beta\mu^2+\ldots\end{aligned} \tag{18}$$

What is the quantum state of a photon pair with detunings μ and $-\mu$ changed by dispersion if they are detected at D_1 and D_2? The quantum state before dispersion is [5,6, 27]

$$|\Psi\rangle = \int d\mu F(\mu)\hat{a}_s^\dagger(\omega_s^0+\mu)\hat{a}_i^\dagger(\omega_i^0-\mu)|0\rangle. \tag{19}$$

After passing the BS, the quantum state becomes

Optics EXPRESS

$$k_s = \frac{\omega_s^0 + \mu}{c}, k_i = \frac{\omega_i^0 - \mu}{c} = \frac{\omega_s^0 - \mu}{c}$$
$$|\Psi\rangle_\mu = e^{i\omega_s^0 \frac{\Delta L}{c}} \left(|\mu\rangle_s |-\mu\rangle_i + e^{-i\mu\frac{2\Delta L}{c}} |-\mu\rangle_s |\mu\rangle_i \right), \quad (20)$$
$$|\Psi'\rangle = \int d\mu F(\mu) |\Psi\rangle_\mu$$

where $|\mu\rangle_s = \hat{a}_s^\dagger(\omega_s^0 + \mu)|0\rangle, |-\mu\rangle_i = \hat{a}_i^\dagger(\omega_i^0 - \mu)|0\rangle$.

How is the quantum state changed if a dispersive medium is placed in the path of the signal photon? The difference between the phase change in vacuum and that in the dispersive medium is given as $(k_s(\mu)-\omega_s/c)L$ and $(k_s(-\mu)-\omega_s/c)L$ for the quantum state of different detunings when the length of the medium is L. Therefore, the quantum state becomes

$$|\Psi\rangle_\mu = e^{i\omega_s \frac{\Delta L}{c}} e^{i\left(k_s(\mu)-\frac{\omega_s}{c}\right)L} |\mu\rangle_s |-\mu\rangle_i + e^{i\left(k_s(-\mu)-\frac{\omega_s}{c}\right)L} e^{-i\mu\frac{2\Delta L}{c}} |-\mu\rangle_s |\mu\rangle_i \quad (21)$$
$$= e^{i\phi(\mu)} |\mu\rangle_s |-\mu\rangle_i + e^{-i\left((k_s(\mu)-k_s(-\mu))L + \frac{2\mu}{c}(\Delta L - L)\right)} |-\mu\rangle_s |\mu\rangle_i$$
$$\left(\phi(\mu) = \frac{\omega_s}{c}(\Delta L - L) + k_s(\mu)\right)$$

after passing through the dispersive medium. Because

$$k_s(\mu) - k_s(-\mu) = k_0 + \alpha\mu + \beta\mu^2 - (k_0 - \alpha\mu + \beta\mu^2), \quad (22)$$
$$= 2\alpha\mu$$

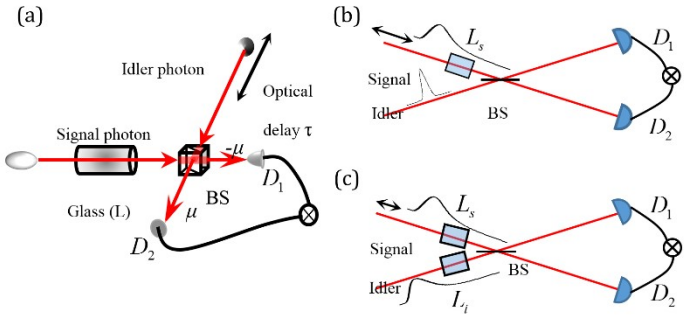

Fig. 6. HOM interference and dispersion cancellation. (a) Dispersion cancellation experiment of Steinberg [1]. The signal photon of the entangled photon pair travels in free space, whereas the idler photon passes through a dispersive material (glass sample L). The two photons meet at the beam splitter(BS), and HOM interference occurs. The shape of the interference pattern is not distorted, and only the position of the dip is shifted. μ, $-\mu$ are detunings from the half-centre frequencies of photons detected at detector 1(D_1) and detec-tor 2(D_2), respectively. (b) The dispersion experiment of Stei-nberg performed with two independent single-photon wave packets. The wave packet is distorted after it passes through the dispersive material. Different from the original experim-ent of Steinberg, dispersive material has strong dispersion property, i.e., high order dispersion coefficients are non-negligible, in this figure. Whether dispersion is weak or strong, dispersion cancellation does not occur because the two wave packets cannot overlap completely at the beam splitter. (c) Two independent and separable wave packets pass through a dispersive material. The dispersion of the two wave packets is identical. Therefore, the two wave packets are indistinguishable at the BS, and the HOM dip is restored without entanglement.

the quantum state can be rewritten as

Optics EXPRESS

$$|\Psi\rangle_{\mu} = e^{i\phi(\mu)}\left(|\mu\rangle_s|-\mu\rangle_i + e^{-i\left(2\mu\left(\frac{\Delta L-L}{c}+\alpha L\right)\right)}|-\mu\rangle_s|\mu\rangle_i\right). \tag{23}$$

The coincidence count for this pair is

$$P_{12}(\mu,-\mu) = \frac{1}{2}\left(1-\cos\left(2\mu\left(\frac{\Delta L-L}{c}+\alpha L\right)\right)\right). \tag{24}$$

When $\Delta L = (1-c\alpha)L$, $P_{12}(\mu,-\mu) = 0$.

As shown above, the phase changes originated from even-order terms in the dispersion relation are identical for both the Reflection-Reflection path and Transmission-Transmission paths. Therefore, these phase changes cancel each other out when the total phase change is calculated. If the dispersion relation is approximated to the second-order terms, only the effect from group velocity remains. The HOM dip resulting from this effect is

$$\begin{aligned} P_{12} &= \frac{1}{2}\int_{-\infty}^{\infty} d\mu |F(\mu)|^2\left(1-\cos\left(2\mu\left(\frac{\Delta L-L}{c}+\alpha L\right)\right)\right) \\ &= \frac{1}{2}\left(1-\int_{-\infty}^{\infty} d\mu |F(\mu)|^2\cos\left(2\mu\left(\frac{\Delta L-L}{c}+\alpha L\right)\right)\right). \end{aligned} \tag{25}$$

and if $\Delta L = (1-c\alpha)L$, then $P_{12} = 0$. In other words, the shape of the HOM dip does not change, and only the position of the lowest point is shifted [1,5].

Appendix B: HOM interference and all-order dispersion cancellation with a separable photon pair

The HOM interference of two separable and independent single photons has been reported [6]. To apply this experiment, we consider the balanced dispersion of two independent single-photon wave packets, as shown in Fig. 6(c). In this setup, the photo detection amplitudes for each wave packet are given as

$$\begin{aligned} \langle 0|\hat{E}_s^{(+)}(z=0,t_1)|\psi\rangle &= g(t_1) \\ \langle 0|\hat{E}_i^{(+)}(z=0,t_2)|\varphi\rangle &= g(t_2) \end{aligned} \tag{26}$$

and satisfy the following equation:

$$\int dt_1 |g(t_1)|^2 = 1, \int dt_2 |g(t_2)|^2 = 1$$

The two photons are generated almost simultaneously; therefore, they have strong temporal correlation. If we write

$$t_{1,s} = t_1 - \frac{L_s}{c}, t_{1,i} = t_1 - \frac{L_i}{c}, t_{2,s} = t_2 - \frac{L_s}{c}, t_{2,i} = t_2 - \frac{L_i}{c},$$

the photo-detection amplitude for the detection of the two photons with D_1 and D_2 is

Optics EXPRESS

$$
\begin{aligned}
|\Psi\rangle &= |\varphi\rangle|\psi\rangle \\
\langle 0|\hat{E}_{D_2}^{(+)}(t_2)\hat{E}_{D_1}^{(+)}(t_1)|\Psi\rangle &= \langle 0|\frac{1}{\sqrt{2}}\left(i\hat{E}_s^{(+)}(t_{2,s})+\hat{E}_i^{(+)}(t_{2,i})\right)\frac{1}{\sqrt{2}}\left(\hat{E}_s^{(+)}(t_{1,s})+i\hat{E}_i^{(+)}(t_{1,i})\right)|\Psi\rangle \\
&= \frac{1}{2}i\langle 0|\hat{E}_s^{(+)}(t_{2,s})\hat{E}_s^{(+)}(t_{1,s})|\Psi\rangle - \frac{1}{2}\langle 0|\hat{E}_s^{(+)}(t_{2,s})\hat{E}_i^{(+)}(t_{1,i})|\Psi\rangle \\
&\quad + \frac{1}{2}\langle 0|\hat{E}_i^{(+)}(t_{2,i})\hat{E}_s^{(+)}(t_{1,s})|\Psi\rangle + \frac{1}{2}i\langle 0|\hat{E}_i^{(+)}(t_{2,i})\hat{E}_i^{(+)}(t_{1,i})|\Psi\rangle \\
&= \frac{1}{2}\langle 0|\hat{E}_i^{(+)}(t_{2,i})\hat{E}_s^{(+)}(t_{1,s})|\Psi\rangle - \frac{1}{2}\langle 0|\hat{E}_s^{(+)}(t_{2,s})\hat{E}_i^{(+)}(t_{1,i})|\Psi\rangle. \\
&= \frac{1}{2}\left(g(t_{2,i})g(t_{1,s})-g(t_{2,s})g(t_{1,i})\right)
\end{aligned}
\tag{27}
$$

In HOM interference, the probability of detecting photons is integrated over time. (In the experiment, the detector is turned on for a finite time. In most cases, the time interval far exceeds the temporal width of the wave packet.) The coincidence count from this integration is

$$
\begin{aligned}
R_{12} &= \iint dt_1 dt_2 \left|\langle 0|\hat{E}_{D_2}^{(+)}(t_2)\hat{E}_{D_1}^{(+)}(t_1)|\Psi\rangle\right|^2 \\
&= \frac{1}{4}\iint dt_1 dt_2 \left|\left(g(t_{2,i})g(t_{1,s})-g(t_{2,s})g(t_{1,i})\right)\right|^2 \\
&= \frac{1}{4}\iint dt_1 dt_2 \left|g(t_{2,i})g(t_{1,s})\right|^2 + \frac{1}{4}\iint dt_1 dt_2 \left|g(t_{2,s})g(t_{1,i})\right|^2 \\
&\quad - \frac{1}{4}\iint dt_1 dt_2 g^*(t_{2,i})g(t_{2,s})g^*(t_{1,s})g(t_{1,i}) - \frac{1}{4}\iint dt_1 dt_2 g(t_{2,i})g^*(t_{2,s})g(t_{1,s})g^*(t_{1,i}). \\
&= \frac{1}{2} - \frac{1}{2}\mathrm{Re}\iint dt_1 dt_2 \left(g^*(t_{2,i})g(t_{2,s})\,g^*(t_{1,s})g(t_{1,i})\right)
\end{aligned}
\tag{28}
$$

As in the case of the entangled photon pair, the coincidence count decreases to 0 when $L_s - L_i = \Delta L = 0$. The distribution of the coincidence count rate is determined by convolution between the photo detection amplitude of each wave packets. When $\Delta L/c$ exceeds the width of the wave packet, the interference effect is not manifested. Therefore, HOM interference can be observed with two separable and independent wave packets.

What happens if we place a dispersion material in one arm of the interferometer, as shown in Fig. 6(b)? Suppose that the photo-detection amplitude of a photon changes from $g(t)$ to $g_d(t)$ after dispersion. Thus, the photo-detection amplitude for two photons becomes

$$
\langle 0|\hat{E}_{D_2}^{(+)}(t_2)\hat{E}_{D_1}^{(+)}(t_1)|\Psi\rangle = \frac{1}{2}\left(g_d(t_2-\frac{L_i}{c})g(t_1-\frac{L_s}{c}) - g(t_2-\frac{L_s}{c})g_d(t_1-\frac{L_i}{c})\right). \tag{29}
$$

Thus, the two photon coincidence count becomes

$$
\iint dt_1 dt_2 \left|\langle 0|\hat{E}_{D_2}^{(+)}(t_2)\hat{E}_{D_1}^{(+)}(t_1)|\Psi\rangle\right|^2 = \frac{1}{2}\left(1-\mathrm{Re}\iint dt_1 dt_2 g_d^*(t_{2,i})g(t_{2,s})g_d^*(t_{1,s})g(t_{1,i})\right). \tag{30}
$$

Dispersion cancellation is not observed.

Consider a balanced dispersion HOM interferometer, as shown in Fig. 6(c), in which each of the two independent wave packets passes through a dispersive material. Although the two wave packets are distorted by dispersion, they can interfere destructively because they have identical temporal amplitude distributions. The effect of dispersion is not manifested in the coincidence count. In this case, the two-photon coincidence count becomes the following:

Optics EXPRESS

$$\iint dt_1 dt_2 \left|\langle 0|\hat{E}_{D_2}^{(+)}(t_2)\hat{E}_{D_1}^{(+)}(t_1)|\Psi\rangle\right|^2 = \frac{1}{2}\left(1-\mathrm{Re}\iint dt_1 dt_2 g_d^*(t_{2,i})g_d(t_{2,s})g_d^*(t_{1,s})g_d(t_{1,i})\right). \quad (31)$$

The formula can be rewritten as follows:

$$\int dt_1 g_d^*(t_{1,s})g_d(t_{1,i}) = \int dt_{1,s} g_d^*(t_{1,s})g_d(t_{1,s}+\frac{L_s-L_i}{c}). \quad (32)$$

This can be expanded as

$$\begin{aligned}
&g(t) = \frac{1}{\sqrt{2\pi}}\int d\omega \bar{g}(\omega)e^{i\omega t}\\
&g_d(t) = \frac{1}{\sqrt{2\pi}}\int d\omega \bar{g}(\omega)e^{-ik(\omega)L}e^{i\omega t}\\
&\int dt_{1,s} g_d^*(t_{1,s})g_d(t_{1,s}+\frac{L_s-L_i}{c})\\
&= \frac{1}{2\pi}\int dt_{1,s}\int d\omega' \bar{g}^*(\omega')e^{ik(\omega')z-i\omega' t_{1,s}}\int d\omega \bar{g}(\omega)e^{-i(k(\omega)L-\omega(t_{1,s}+\frac{L_s-L_i}{c}))}\\
&= \frac{1}{2\pi}\int d\omega'\int d\omega\int dt_{1,s}\bar{g}^*(\omega')\bar{g}(\omega)e^{i(k(\omega')-k(\omega))L}e^{i(\omega(t_{1,s}+\frac{L_s-L_i}{c})-\omega' t_{1,s})}\\
&= \frac{1}{2\pi}\int d\omega'\int d\omega\bar{g}^*(\omega')\bar{g}(\omega)e^{i(\omega\frac{L_s-L_i}{c})}e^{i(k(\omega')-k(\omega))L}\int dt_{1,s}e^{i(\omega-\omega')t_{1,s}}\\
&= \frac{1}{2\pi}2\pi\int d\omega'\int d\omega\bar{g}^*(\omega')\bar{g}(\omega)e^{i(\omega\frac{L_s-L_i}{c})}e^{i(k(\omega')-k(\omega))L}\delta(\omega-\omega')\\
&= \int d\omega|\bar{g}(\omega)|^2 e^{i(\omega\frac{L_s-L_i}{c})}
\end{aligned} \quad (33)$$

The result does not depend on $k(\omega)$; therefore, the same result is achieved, even in the absence of dispersion.

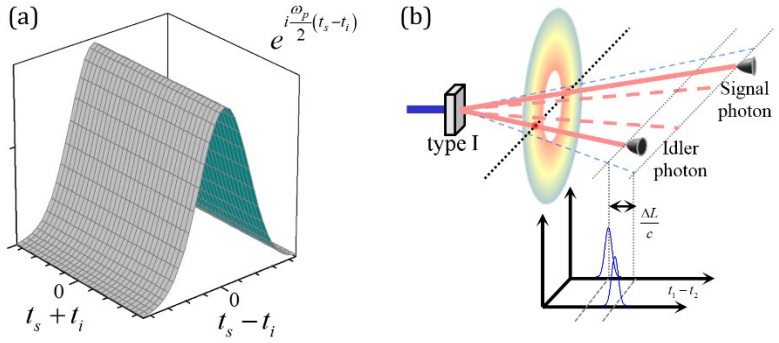

Fig. 7. (a) Biphoton wave packet. If t_s-t_i has the same value, the photons are detected with the same probability, regardl-ess of t_s, t_i. The amplitudes at different times exhibit only a phase difference. The amplitudes at different times exhibit two-photon mutual temporal coherence. (b)If the signal and idler photons travel different distances, the temporal distribution of the amplitude is shifted. The shift is determined by the length of the path difference.

$$\int dt_1 g_d^*(t_{1,s})g_d(t_{1,i}) = \int dt_{1,s} g^*(t_{1,s})g(t_{1,s}+\frac{L_s-L_i}{c}). \quad (34)$$

Optics EXPRESS

The same principle applies to $g_d(t_{2,s})$. The HOM interference pattern is restored by this process. Therefore, even if two photons are not entangled, the dispersion effect is not manifested.

Appendix C: biphoton wave packet in HOM interference and all-order dispersion cancellation

A biphoton wave packet is the amplitude distribution of an energy-time entangled photon pair in the time domain. An energy-time entangled state satisfies the inequality $\Delta(t_s - t_i)\Delta(\omega_s + \omega_i - \omega_p) \le 1$, where t_s and t_i are the detection times for the signal and idler photons, respectively; and ω_s, ω_i, ω_p are the angular frequencies of the signal, idler, and pump beams, respectively. In other words, the photon pair has strong temporal correlation and strong frequency anti-correlation. The frequency anti-correlation makes a biphoton wave packet differ substantially from the wave packets of a photon pair with classical correlation. The temporal distribution of the photo detection amplitude from this quantum state has the following form [27]:

$$\left\langle 0 \left| \hat{E}_s^{(+)}(t_s)\hat{E}_i^{(+)}(t_i) \right| \Psi \right\rangle = e^{i\frac{\omega_p}{2}(t_s+t_i)} g(t_s - t_i). \tag{35}$$

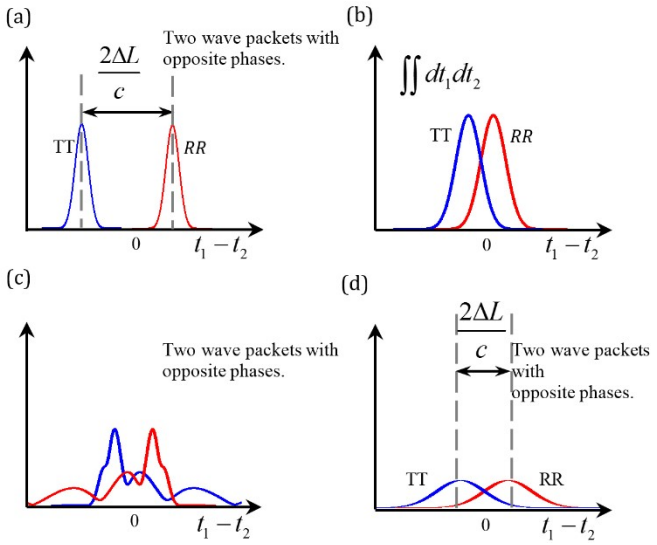

Fig. 8. (a) Photo-detection amplitude distribution along the t_1-t_2 axis. The wave packets from the RR and TT paths are shifted in the opposite directions and are anti-symmetric around the t_1-t_2 = 0 point. The two wave packets have opposite phase, and the whole wave packet is the superposition of the two wave packets. (b) If the path length difference is decreased, the two wave packets overlap. The overlapping region causes interference terms, and the coincidence count rate is changed. This results in HOM interference. When the path length difference is 0, the two wave packets overlap completely and cancel each other out. Thus, the coincidence count rate is 0. (c) HOM interference after dispersion. Because the amplitudes of the TT and RR paths are asymmetric, they do not interfere completely. Thus, the interference pattern is distorted. (d) HOM interference after odd-order dispersion cancellation. Because two wave packets with even-order dispersion have symmetric distributions, complete destructive interference occurs when the path length difference is 0.

The character of this temporal distribution clearly differs from that of the temporal distribution of classically correlated wave packets. If $t_s - t_i$ is the same, the probability of detecting photons is the same, regardless of t_s, t_i. If $t_s - t_i$ has the same value, the photo-detection amplitudes at different times have the same magnitude. Only the phase is different,

Optics EXPRESS

and a perfect temporal coherence exists between the photo-detection amplitudes at different times. Fig. 7(a) presents this distribution.

How does this distribution change after the photon pair passes through the BS of the HOM interferometer? The change in the amplitude distribution after the signal and idler photons travel finite distances answers this question. When the distance the signal photon travels is L_s and that of the idler photon is L_i, a difference exists between the photon generation time and the detection time. Thus, if a signal photon is detected at t_1, it was generated at time $t_1' = t_1 - L_s / c$ .Therefore, if the signal and idler photons are detected at t_1 and t_2, respectively, then the photo detection amplitude is

$$\begin{aligned}\left\langle 0\left|\hat{E}_s^{(+)}(t_1)\hat{E}_i^{(+)}(t_2)\right|\Psi\right\rangle &= e^{i\frac{\omega_p}{2}(t_1+t_2-\frac{L_s}{c}-\frac{L_i}{c})}\, g(t_1-\frac{L_s}{c}-t_2+\frac{L_i}{c}) \\ &= e^{i\frac{\omega_p}{2}(t_1+t_2-\frac{L_s+L_i}{c})}\, g(t_1-t_2-\frac{\Delta L}{c}).\end{aligned} \tag{36}$$

$$\Delta L = L_s - L_i$$

This distribution is shifted by $\Delta L/c$ from the original distribution of the biphoton wave packet along the t_1–t_2 axis. When the two path lengths of the HOM interferometer are different, the photo-detection amplitudes at D_1 and D_2 are also shifted. If the photon pair follows the reflection-reflection path at the BS, this behaviour corresponds to the signal-D_2, idler-D_1 path. In contrast, if the pair follows the transmission-transmission path, they move along the signal- D_1 idler- D_2 path .Thus, the wave packet from each path is in the opposite direction and is anti-symmetric around the t_1- t_2 = 0 point.

If a biphoton wave packet from the RR path has a distribution $g'(t_1 - t_2 - \Delta L / c)$, the biphoton wave packet from the TT path has a distribution $-g'(-(t_1 - t_2 - \Delta L / c))$. The minus (–) sign in front of the distribution originates from the phase difference between the RR and TT paths. The whole wave packet of the photon pair is a superposition of the two wave packets.

What happens if a dispersion material is placed in one of the paths? When the dispersion is very strong, the shape of the biphoton wave packet is asymmetrically distorted because of odd-order dispersion (Fig. 9(a)).

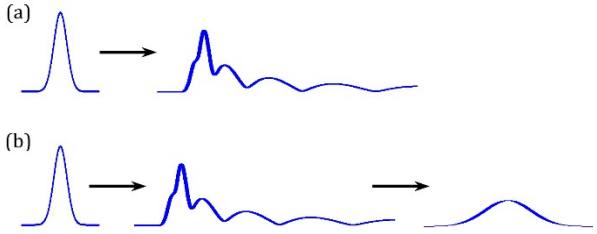

Fig. 9. (a) If a Gaussian wave packet passes through a medium with strong dispersion, the wave packet becomes distorted. Additionally, because of odd-order dispersion, the shape of the wave packet becomes asymmetrical. (b) Nonlocal dispersion cancellation of odd-order dispersion. When only one photon passes through a dispersive material, the biphoton wave packet is distorted. If another photon also passes through an identical dispersive material, then odd-order dispersion is cancelled out because of frequency anti-correlation. Thus, only the even-order dispersion effect remains, and the wave packets become symmetric.

The photo-detection amplitude at D_1 and D_2 becomes the distribution shown in Fig. 8(c). Because the two wave packets are anti-symmetric around the t_1- t_2 =0 point, they cannot overlap completely. Thus, complete destructive interference cannot occur, and the HOM dip is distorted. If dispersion is balanced at both paths, then nonlocal dispersion cancellation

Optics EXPRESS

occurs for odd-order dispersion. If one photon passes through a dispersive material, the biphoton wave packet is distorted. If another photon also passes through an identical dispersion material, then odd-order dispersion is cancelled out, and only the even-order dispersion effect remains (Fig. 9(b)). As demonstrated by Steinberg [13], even-order dispersion does not change the shape of the interference pattern for HOM interference. Therefore, the interference pattern without dispersion is restored. The wave packet distribution for this process is shown in Fig. 8(d).

How does this apply in the case of a modified HOM interferometer with a Mach-Zender interferometer? Because a biphoton wave packet does not have a definite generation time, the two-photon amplitudes generated earlier and later have mutual temporal coherence. If the advanced amplitude propagates over a longer path, the two amplitudes can meet at the detectors and interfere. If the temperature of the cell is so low that the dispersion effect is negligible, the distribution of the wave packet is like that shown in Fig. 10(a). When $L_0=(L_{Long}+L_{Short})/2$, the wave packets connected by the arrow overlap and interfere. If the temperatures of the two cells are high and different, then unbalanced dispersion occurs. Because wave packets from the RR and TT paths are distributed asymmetrically, the total distribution is modified. Because the two wave packets connected by arrows have different distributions, destructive interference cannot occur completely. If the temperatures of the two cells are balanced, then nonlocal odd-order interference pattern without dispersion is restored. Throughout this process, energy-time dispersion cancellation occurs. Only the even-order dispersion effect remains. Thus, the entanglement affect the interference two times.

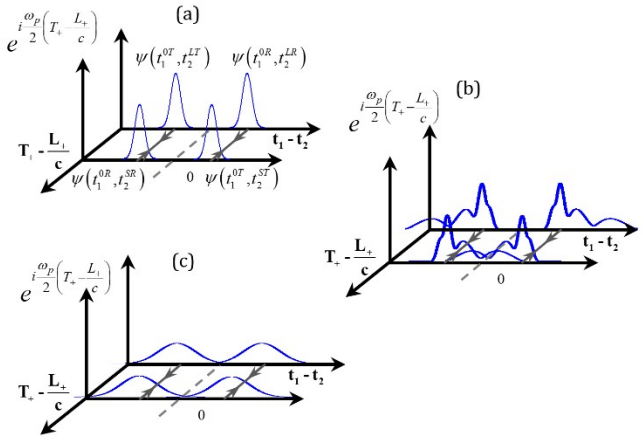

Fig. 10. (a) Biphoton wave packet distribution after the BS when $L_0 = (L_{Long} + L_{Short})/2$ in modified HOM inteference. The arrow indicates that the amplitude generated earlier and the amplitude generated later meet and interfere. The amplitude generated earlier, which travelled along the TT path, interferes with the amplitude generated later that travelled along the RR path and vice versa. $T_+ = t_1 + t_2$ and L_+ denotes sum of signal path length and idler path length. $L_+ = L_s + L_i$. (b) Biphoton wave packet after the BS in the presence of a dispersive material. The amplitudes that travelled along the TT and RR paths do not overlap completely. Constructive or destructive interference cannot occur completely, and the interference pattern is distorted. (c) Biphoton wave packet after the BS with balanced dispersion. Because the wave packets are symmetric, the amplitudes that travelled along the TT and RR paths overlap completely. Thus, constructive or destructive interference can occur completely, and the interference pattern is restored.

Frequency anti-correlation makes the temporal information of the photon pair uncertain. Two-photon temporal coherence originates from this property and enables interference between the wave packets, as shown in Fig. 10. The nonlocal cancellation of odd-order dispersion also originates from frequency anti-correlation. In the absence of any of these processes, all-order dispersion cancellation in the modified HOM interferometer cannot

Optics EXPRESS

occur. None of these processes occur with two single-photon wave packets with classical temporal correlation

Appendix D: measuring the degree of asymmetry with the visibility of HOM interference

Effect of dispersion in HOM interference can be treated more quantitatively. The distortion of the two-photon interference pattern reflects the odd-order dispersion of a biphoton wave packet. We can determine the degree of odd-order dispersion based on the visibility of the interference dip or peak. As shown in Fig. 9, asymmetric distortion occurs via odd-order dispersion. We can quantitatively determine the degree of asymmetry of the wave function via a simple integration. Suppose that $\varphi(t)$ is an asymmetric wave function. $\varphi(-t)$ is a function that is mirror symmetric with $\varphi(t)$ around t=0. To show the asymmetry quantitatively, we can decompose $\varphi(t)$ to a symmetric function and an anti-symmetric function as shown below. The two functions are normalised.

$$\begin{aligned}
&\int_{-\infty}^{\infty} dt\left|\varphi(t)\right|^2 = 1 \\
&\varphi(t) = a\varphi_s(t) + b\varphi_A(t) \\
&\varphi_s(-t) = \varphi_s(t), \int_{-\infty}^{\infty} dt\left|\varphi_s(t)\right|^2 = 1. \\
&\varphi_A(-t) = -\varphi_A(t), \int_{-\infty}^{\infty} dt\left|\varphi_A(t)\right|^2 = 1
\end{aligned} \tag{37}$$

If $\varphi(t)$ has perfect symmetry or anti-symmetry, then $\left||a|^2 - |b|^2\right| = 1$ .However, this value is far smaller than 1 if $\varphi(t)$ is quite asymmetric. Therefore, $1-\left||a|^2 - |b|^2\right|$ can reflect the degree of asymmetry(*D.A.*). It is not necessary to obtain a and b directly to calculate *D.A.* Indeed, *D.A.* can be calculated from $\varphi(t)$ and $\varphi(-t)$ as follows:

$$\begin{aligned}
\int_{-\infty}^{\infty} dt\varphi(t)\varphi^*(-t) &= \int_{-\infty}^{\infty} dt\left(a\varphi_s(t) + b\varphi_A(t)\right)\left(a\varphi_s(-t) + b\varphi_A(-t)\right)^* \\
&= \int_{-\infty}^{\infty} dt\left(a\varphi_s(t) + b\varphi_A(t)\right)\left(a\varphi_s(t) - b\varphi_A(t)\right)^* \\
&= \int_{-\infty}^{\infty} dt\left(\left|a\varphi_s(t)\right|^2 - \left|b\varphi_A(t)\right|^2 + ab^*\varphi_s(t)\varphi_A(t)^* + a^*b\varphi_s(t)^*\varphi_A(t)\right). \\
&= \int_{-\infty}^{\infty} dt\left(\left|a\varphi_s(t)\right|^2 - \left|b\varphi_A(t)\right|^2\right) \\
&= |a|^2 - |b|^2
\end{aligned} \tag{38}$$

$$D.A. = 1 - \left|\int_{-\infty}^{\infty} dt\varphi(t)\varphi^*(-t)\right| = 1 - \left||a|^2 - |b|^2\right|$$

For an asymmetric wave function,

$$\left|\int_{-\infty}^{\infty} dt\varphi(t)^*\varphi(-t)\right| < 1. \tag{39}$$

is always true. In other words, *D.A.*>*0.*

More asymmetric functions are correlated with higher *D.A.* values. However, $\varphi(t)$ and $\varphi(-t)$ can have a relationship in the form of $\varphi(-t)=\varphi(t+t_0)$, where t_0 is a fixed value. In this case, the integral described above is less than 1, but it does not accurately reflect the degree of distortion. Thus, we consider a function that has the form of a convolution:

Optics EXPRESS

$$v(\tau)=\int_{-\infty}^{\infty}dt\varphi^{*}(t+\tau)\varphi(-t). \tag{40}$$

If $\varphi(-t)=\varphi(t+t_0)$, then $v(\tau)=1$ when $\tau=t_0$. However, if $\varphi(t)$ is asymmetric and $\varphi(-t)\neq\varphi(t+t_0)$ for any value of τ, then $v(\tau)$ is always $v(\tau)<1$. The maximum value of $v(\tau)$ must be found by varying the value of τ. This property can be applied to both HOM interference and modified HOM interference. The effective photon wave function for an energy-time entangled pair has the following form:

$$\Phi(t_1,t_2)=e^{i\omega_p(t_1+t_2)}g(t_1-t_2). \tag{41}$$

The effective wave functions for transmission-transmission path and reflection-reflection path are

$$\begin{aligned}\Phi_{TT}(t_1,t_2)&=\frac{1}{\sqrt{2}}e^{i\omega_p(t_1+t_2)}g(t_1-t_2)\\ \Phi_{RR}(t_1,t_2)&=-\frac{1}{\sqrt{2}}e^{i\omega_p(t_1+t_2)}g(-(t_1-t_2)).\\ \int dt\left|g(t)\right|^2&=1\end{aligned} \tag{42}$$

The visibility is determined by the product of two functions.

$$V=\left|-\frac{2}{T}\mathrm{Re}\left(\int_0^T dt_1\int_0^T dt_2\Phi_{TT}^{*}(t_1,t_2)\Phi_{RR}(t_1,t_2)\right)\right|. \tag{43}$$

Since temporal width of the wave packet is far narrower than T, (16)-(20) can also be applied to the visibility.

$$\begin{aligned}V&=\left|\frac{1}{T}\mathrm{Re}\left(\int_0^T dt_1\int_0^T dt_2 g^{*}(t_1-t_2)g(-(t_1-t_2))\right)\right|\\ &=\left|\mathrm{Re}\left(\int dt_{-}g^{*}(t_{-})g(-t_{-})\right)\right|.\end{aligned} \tag{44}$$

,where $t_{-}=t_1-t_2$.

As (38) shows, $\int dt_{-}g^{*}(t_{-})g(-t_{-})$ is always a real value. Thus, we can rewrite (43) as

$$V=\left|\int dt_{-}g^{*}(t_{-})g(-t_{-})\right|. \tag{45}$$

The visibility cannot be $V=1$ if the wave function is asymmetric. For a more asymmetric wave function, the visibility has a smaller value. *D.A.* can be calculated as

$$D.A.=1-V. \tag{46}$$

Funding

This work was supported by National Research Foundation of Korea (NRF) grants funded by the "Ultrashort Quantum Beam Facility Program" and partly by "The Project of Conversion by the Past R&D Results" through the Ministry of Trade, Industry and Energy (MOTIE) and the Korea Institute for the Advancement of Technology (KIAT) (N0001541, 2015)